AIP | The Journal of Chemical Physics

Surface forces: Surface roughness in theory and experiment

Drew F. Parsons, Rick B. Walsh, and Vincent S. J. Craig

Citation: The Journal of Chemical Physics **140**, 164701 (2014); doi: 10.1063/1.4871412
View online: http://dx.doi.org/10.1063/1.4871412
View Table of Contents: http://scitation.aip.org/content/aip/journal/jcp/140/16?ver=pdfcov
Published by the AIP Publishing

Articles you may be interested in

Reconstruction of reverberation levels based on measured surface roughness: Theory and experiment.
J. Acoust. Soc. Am. **129**, 2510 (2011); 10.1121/1.3588296

Solvation forces between rough surfaces
J. Chem. Phys. **108**, 5588 (1998); 10.1063/1.475973

Surface roughness determination using the acousto-optic technique: Theory and experiment
Appl. Phys. Lett. **71**, 599 (1997); 10.1063/1.119805

A surface enhanced resonance Raman study of cobalt phthalocyanine on rough Ag films: Theory and experiment
J. Chem. Phys. **87**, 4189 (1987); 10.1063/1.452923

Forward and specular scattering from a rough surface: theory and experiment
J. Acoust. Soc. Am. **53**, 791 (1973); 10.1121/1.1913394

AIP | Journal of Applied Physics

Journal of Applied Physics is pleased to announce André Anders as its new Editor-in-Chief

This article is copyrighted as indicated in the article. Reuse of AIP content is subject to the terms at: http://scitation.aip.org/termsconditions. Downloaded to IP: 150.203.177.24 On: Wed, 23 Jul 2014 23:40:58

Surface forces: Surface roughness in theory and experiment

Drew F. Parsons,[a] Rick B. Walsh, and Vincent S. J. Craig
Department of Applied Mathematics, Research School of Physical Sciences and Engineering, Australian National University, Canberra, ACT 0200, Australia

(Received 20 January 2014; accepted 3 April 2014; published online 22 April 2014)

A method of incorporating surface roughness into theoretical calculations of surface forces is presented. The model contains two chief elements. First, surface roughness is represented as a probability distribution of surface heights around an average surface height. A roughness-averaged force is determined by taking an average of the classic flat-surface force, weighing all possible separation distances against the probability distributions of surface heights. Second the model adds a repulsive contact force due to the elastic contact of asperities. We derive a simple analytic expression for the contact force. The general impact of roughness is to amplify the long range behaviour of noncontact (DLVO) forces. The impact of the elastic contact force is to provide a repulsive wall which is felt at a separation between surfaces that scales with the root-mean-square (RMS) roughness of the surfaces. The model therefore provides a means of distinguishing between "true zero," where the separation between the average centres of each surface is zero, and "apparent zero," defined by the onset of the repulsive contact wall. A normal distribution may be assumed for the surface probability distribution, characterised by the RMS roughness measured by atomic force microscopy (AFM). Alternatively the probability distribution may be defined by the histogram of heights measured by AFM. Both methods of treating surface roughness are compared against the classic smooth surface calculation and experimental AFM measurement. © *2014 AIP Publishing LLC*. [http://dx.doi.org/10.1063/1.4871412]

I. INTRODUCTION

The DLVO theory of colloidal stability, developed by Derjaguin and Landau,[1] Verwey and Overbeek,[2] has been of considerable value in understanding surface interactions between colloidal particles immersed in a liquid. While the limitations of the theory are well known,[3–5] the theory has nevertheless provided insight across a vast range of fields, including agriculture and food science,[6–8] mineral and oil extraction,[9,10] and filtration[11] and biology.[12–14]

One limitation of the theory is that it is built upon the assumption of ideally smooth surfaces. The boundaries between surfaces and solution are taken to be infinitesimally sharp, with the separation distance between surfaces uniquely defined by a single value L. In practice real surfaces are typically never atomically smooth but are characterised by a certain roughness, with pits and mounds causing the local surface height to deviate around its average value. Consequently the surface forces calculated between purely smooth surfaces by DLVO theory do not in general provide the most accurate estimate of the real surface forces.[15–17] As various locations across the surface rise or fall in accordance with that surface's roughness, the local distance between the two surfaces becomes greater or smaller, perturbing the force felt between surfaces. Note here we focus on particles immersed in a liquid phase and therefore do not consider capillary forces. The treatment of capillary forces in a similar manner would require the use of a force law that described how the force changes with separation of the particles.[18–20]

Surface roughness thus alters the noncontact force away from that predicted for smooth surfaces. At the same time roughness introduces asperities which come into contact long before the average positions of the two surfaces make contact at $L = 0$. The elastic contact of smooth surfaces is already employed to describe a repulsive contact wall at $L = 0$ using the Hertzian theory of contact of macroscopically curved surfaces (that is, with radius of curvatures of the order of μm),[21–23] or with enhancements added by Johnson, Kendall, and Roberts (JKR theory[24]) or by Derjaguin, Muller, and Toporov (DMT theory[25]) to account for adhesive contact.[26,27] We apply elastic contact at a microscopic level, that is, to contact between asperities. The elastic contact of tall asperities, although covering only a fraction of the total surface, generates a repulsive contact force which forms an effectively impenetrable wall at nonzero separation $L > 0$.

In this way, our model contains two chief elements, the roughened noncontact force and the elastic contact of asperities. We obtain these two quantities by employing a statistical description of surface roughness, averaging both the noncontact force of conventional smooth-surface theory and asperity contact force over all statistically possible surface heights.

The procedure is conceptually the same as the Derjaguin approximation, used routinely in colloid science to estimate the forces between curved surfaces from the force calculation (more precisely, the interaction energy) between flat surfaces.[28–30] In the Derjaguin approximation the flat-plate interaction is convolved across a specified geometry (a curved geometry). In our method, the flat-plate interaction is convolved across a probability distribution of surface heights. This approach has been applied to the undulations or surface

[a]Electronic mail: Drew.Parsons@anu.edu.au

 © 2014 AIP Publishing LLC

This article is copyrighted as indicated in the article. Reuse of AIP content is subject to the terms at: http://scitation.aip.org/termsconditions. Downloaded to IP: 150.203.177.24 On: Wed, 23 Jul 2014 23:40:58

fluctuations found in soft matter, enabling soft matter surface forces to be estimated from calculations of their rigid surface counterparts.[31] In some studies a description of surface roughness has been added to DLVO calculations as a modification of surface geometry,[32–36] as variation of the Derjaguin approximation[35,37] or as an additional empirical force.[38,39] The effect of regular (non-random) roughness has been considered through contact of hemispherical asperities.[40] Other studies have introduced a statistical description of roughness into calculation of the van der Waals interaction.[41–44] Advanced statistical analysis of asperity contact has been performed[44,45] but requires detailed knowledge of the surface roughness, not routinely available, and not in combination with roughened noncontact forces. Our model of contact requires only a single asperity parameter (the thickness or curvature of asperities) to be determined, and can be described by explicit analytical formulae. To our knowledge the application of a statistical description of roughness containing both the full noncontact force (e.g., to obtain a roughened DLVO force including both van der Waals attraction and electrolytic repulsion) and the elastic contact of asperities with analytic expressions, has not previously been done.

II. MODELLING ROUGHNESS

We construct our model of roughness in conjunction with the Derjaguin approximation, which estimates the force $F(L)$ between curved surfaces from a calculation of the interaction free energy $G(L)$ between flat, parallel surfaces. For the case of the atomic force microscope (AFM) geometry of an interaction between a sphere of radius r and a flat plane, or the surface forces apparatus (SFA) geometry of crossed cylinders of radius r, the Derjaguin approximation is

$$F(L)/r = 2\pi G(L). \tag{1}$$

In the same spirit as the Derjaguin approximation, our model seeks to estimate the interaction energy $G(L)$ between two rough but flat (parallel) surfaces, based on the interaction energy $G_{\text{smooth}}(L)$ between two smooth, flat surfaces. We then apply the Derjaguin approximation to the rough surface interaction energy to obtain the force between curved surfaces. Our model therefore neglects lateral effects of roughness which might arise due to motion of the surfaces that results in torsional or lateral forces such as would be evident in sliding or rolling.[46,47] Lateral effects may provide corrections of 5% or more at separations less than 200 nm.[48]

Roughness may be accounted for by taking the probability distribution of the height of each surface. Conceptually, the surface is divided into infinitesimal unit areas, with the height of the unit surface placed at z_1 for the first surface and z_2 for the second. These heights vary from one surface element to another according to the respective roughness probability distributions of each surface. Each combination of heights z_1 and z_2 contributes an energy $G_{\text{smooth}}(h)$, where the surface elements are separated by distance $h = z_2 - z_1$. An illustration of the two rough surfaces is represented in Fig. 1.

We account mathematically for the roughness of surface 1 by considering the probability distribution $P_1(z_1)$ of the height of the surface, centred around the average height $\bar{z_1}$.

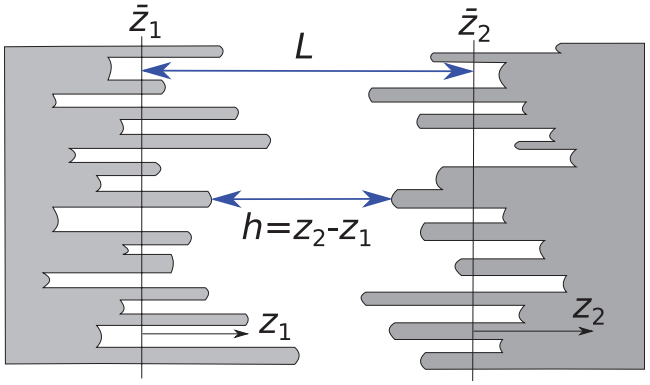

FIG. 1. Illustration of two rough surfaces at average separation L.

The probability distribution may be characterised by the root-mean-square (RMS) roughness σ_1 measured by atomic force microscope. Similarly $\bar{z_2}$ is the average position of the second surface. The average separation L between the two surfaces would then be $L = \bar{z_2} - \bar{z_1}$. We may assume without loss of generality that $\bar{z_1} = 0$ and $\bar{z_2} = L$

The total interaction energy $G(L)$ between the rough surfaces is then a convolution of the smooth-surface interaction energy across the two probability distributions. That is, the total energy is the average over the weighted contributions of all possible values of z_1 and z_2,

$$G(L)\int_{-\infty}^{\infty}\int_{-\infty}^{\infty} dz_1 dz_2 P_1(z_1)P_2(z_2)G_{\text{smooth}}(z_2 - z_1). \tag{2}$$

This roughness-averaged interaction energy may be more simply treated[49] as an average over a single mean height distribution $P_m(h)$,

$$G(L)\int_{-\infty}^{\infty} dh\, P_m(h)G_{\text{smooth}}(h + L), \tag{3}$$

where the mean probability distribution is defined as

$$P_m(h) = \int_{-\infty}^{\infty} dz_1 P_1(z_1)P_2(z_1 + L + h). \tag{4}$$

It is often convenient to assume that the height distributions follow a normal distribution with root mean square roughnesses σ_1 and σ_2, respectively. In this case, $P_1(z_1) = \exp[-(z_1 - \bar{z_1})^2/2\sigma_1^2]/(\sigma_1\sqrt{2\pi})$, and similarly for $P_2(z_2)$. The mean probability distribution then also follows a normal distribution

$$P_m(h) = \frac{\exp\left(-h^2/2\sigma_m^2\right)}{\sigma_m\sqrt{2\pi}}, \tag{5}$$

with mean roughness

$$\sigma_m = \sqrt{\sigma_1^2 + \sigma_2^2}. \tag{6}$$

1. Characterisation of roughness by histogram

A surface with non-normal distribution of heights may be better represented by a histogram $\{H_{1i}\}$ of heights $\{h_{1i}\}$ measured for instance by AFM, rather than a Gaussian RMS

This article is copyrighted as indicated in the article. Reuse of AIP content is subject to the terms at: http://scitation.aip.org/termsconditions. Downloaded to IP: 150.203.177.24 On: Wed, 23 Jul 2014 23:40:58

roughness. Similarly $\{H_{2j}\}$ over heights $\{h_{2j}\}$ defines a histogram for the second surface. The mean heights $\bar{h_1}$ and $\bar{h_2}$ generally have an arbitrary value. The roughness formula, Eq. (2), then becomes

$$G(L) = \frac{1}{N_1 N_2} \sum_i \sum_j H_{1i} H_{2j} G_{\text{smooth}}(h_{2j} - h_{1i} - \bar{h_2} + \bar{h_1} + L), \tag{7}$$

where N_1 is the normalisation factor $N_1 = \sum_i H_{1i}$, similarly for N_2.

As for a continuous distribution, the two histograms may be merged into a single mean histogram $\{H_k\}$ over heights $\{h_k\}$. Here each index k corresponds to one ij pair from the two original histograms, such that $h_k = h_{2j} - h_{1i} - \bar{h_2} + \bar{h_1}$ and $H_k = H_{1i}H_{2j}$. The histogram formula may then be represented as a sum over the single mean histogram,

$$G(L) = \frac{1}{N} \sum_k H_k \, G_{\text{smooth}}(h_k + L), \tag{8}$$

where $N = N_1 N_2$.

Fast computation of Eq. (3) with a normal distribution can be attained by approximating the Gaussian function with a histogram and applying Eq. (8). We find a sufficiently good approximation can be made with a histogram of 501 points spread between $-10\sigma_m$ and $+10\sigma_m$.

A. Asperities in contact: Elastic contact

The classic noncontact smooth surface interaction energy $G_{\text{smooth}}(l)$ that we started with (for instance the interaction energy from DLVO theory) is, strictly speaking, only defined when the surfaces are separated, i.e., when $l > 0$ (l being the separation between flat, smooth surfaces). In the opposite case where $l < 0$, the surfaces have moved past the point of contact. Physically this corresponds to asperities in contact, compressing the surface at those points. A sophisticated analysis of this situation has been performed using perturbation theory, but is complicated by the requirement that the second order roughness response function must be known.[44] A simpler method is to treat contact when $l < 0$ as elastic contact.

The cleanest approach is to include the elastic energy G_{elastic} of asperities in contact as an additive term alongside the usual flat surface noncontact interaction energy for $l > 0$, which we denote as $G_{\text{noncontact}}(l)$. When the surfaces are in contact at $l < 0$, we assume that the noncontact energy remains at its contact value $G_0 = G_{\text{noncontact}}(0)$. Similarly when the surfaces are not in contact at $l > 0$ then the contact energy is zero.

We can then write the total interaction energy between smooth surfaces as

$$G_{\text{smooth}}(l) = G^*_{\text{noncontact}}(l) + G^*_{\text{contact}}(l). \tag{9}$$

The star symbols in $G^*_{\text{noncontact}}$ and G^*_{contact} here mark the special conditions with respect to $l < 0$ or $l > 0$. Specifically,

$$G^*_{\text{noncontact}}(l) = \begin{cases} G_0 & l < 0 \\ G_{\text{noncontact}}(l) & l > 0 \end{cases}, \tag{10}$$

where $G_{\text{noncontact}}(l)$ is the conventional interaction energy (e.g., DLVO energy) between flat, smooth surfaces:

$$G^*_{\text{contact}}(l) = \begin{cases} W_{\text{elastic}}(-l) & l < 0 \\ 0 & l > 0 \end{cases}. \tag{11}$$

$W_{\text{elastic}}(x)$ here refers to the elastic work performed by compressing the asperities through a deformation of $x = -l$. This approach may be compared to the elastic foundation model,[50] which considers elastic contact between individual springs distributed evenly across a smooth surface (with equal heights) interacting only when contact is made. Our model is similar, but takes the height of each "spring" to be variable, such that contact of different springs across the surface occurs at different positions.

A physically intuitive model is to consider asperities as a series of hemispherical peaks, characterised by a radius of curvature R. The elastic contact of two such curved surfaces is described by the contact theory of Hertz.[21] As mentioned above, Hertzian compression has been applied in the interpretation of surface force measurements in order to consider the contact of surfaces at a macroscopic scale after separation L has passed zero.[22,23] It has also been applied at the microscopic level of asperity contact for the kind of randomly rough surfaces which we consider here,[45] but without consideration of non-contact (e.g., DLVO) forces. We consider it unnecessary to add here the further Hertzian contact enhancements of JKR theory[24] or DMT theory.[25] Those enhancements account for adhesive contact[26,27] and are better included in the G_0 term of Eq. (10).

The hemispherical asperity model of Hertzian contact applies naturally to relatively smooth surfaces whose asperities have low aspect ratio (height/base diameter). Under high aspect ratios asperities may be considered as a series of columns extending out perpendicularly from the average surface. In this context Hertzian contact is understood to mean contact between hemispherical caps of such columns.

For asperities with particularly high aspect ratio, say nanowires or stiff polymers with a length scale of a μm,[51,52] asperity bending could be invoked instead of Hertzian compression. The theory of beam bending requires asperities to be characterised by their average thickness (cross-sectional area), rather than their radius of curvature at contact. An "ideal aspect ratio" can be determined, at which Hertzian compression behaves similarly to simple column compression. This case is interesting since it requires no additional asperity parameter (such as the radius of curvature used in Hertzian compression). But Hertzian compression is sufficient for describing asperity contact between rough surfaces over a wide range of typical aspect ratios. We therefore do not consider the other two models in this manuscript, but offer their details in the supplementary material.[66]

1. Hertzian compression of asperities

Hertzian compression is illustrated in Fig. 2. Suppose the hemispherical caps of the asperities of each surface have a radius of curvature R_1 and R_2, respectively. When these asperities are compressed through a distance x, the elastic potential

This article is copyrighted as indicated in the article. Reuse of AIP content is subject to the terms at: http://scitation.aip.org/termsconditions. Downloaded to IP: 150.203.177.24 On: Wed, 23 Jul 2014 23:40:58

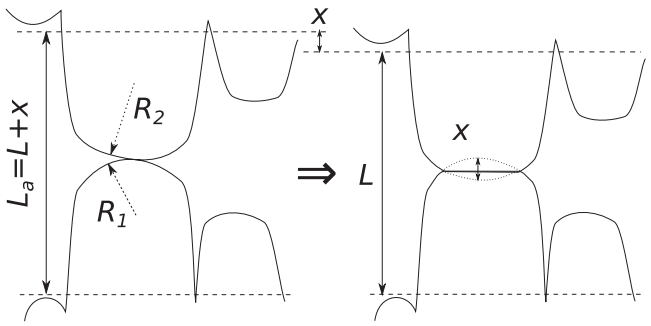

FIG. 2. Illustration of two spherical asperities in contact (Hertzian compression).

energy is[21] $x^{5/2}(8/15)E_r\sqrt{R_r}$. Here R_r is the reduced radius

$$\frac{1}{R_r} = \frac{1}{R_1} + \frac{1}{R_2} \tag{12}$$

and E_r is the reduced Young's modulus,

$$\frac{1}{E_r} = \frac{1-\nu_1^2}{E_1} + \frac{1-\nu_2^2}{E_2}. \tag{13}$$

This contact energy is spread across a contact area $\pi x R_r$. The Hertzian elastic contact work per unit area for a given asperity contact is therefore

$$W_{\text{elastic}}(x) = \frac{8E_r}{15\pi}\frac{x^{3/2}}{\sqrt{R_r}}. \tag{14}$$

We average this elastic contact energy over all asperities by applying this energy (via Eq. (11) in order to allow only positive contact) in Eq. (3). With the roughness of the two surfaces represented by a Gaussian distribution with mean rms roughness $\sigma_m = \sqrt{\sigma_1^2 + \sigma_2^2}$, the total interaction energy of Hertzian elastic contact is

$$G_{\text{contact}}(L) = \frac{2E_r\sigma_m}{15\pi\sqrt{\pi}}\sqrt{\frac{\sigma_m}{R_r}}\exp\left(-\frac{L^2}{4\sigma_m^2}\right) f\left(\frac{L}{\sigma_m}\right). \tag{15}$$

Here we define $f(x) = \sqrt{x}[(1+x^2)K_{(1/4)}(x^2/4) - x^2 K_{(3/4)}(x^2/4)]$. The two $K_n(x)$ functions ($n = \frac{1}{4}$ and $\frac{3}{4}$) are modified Bessel functions of the second kind, which are commonly available (often written as "BesselK") in computer programming libraries. If needed, $f(x)$ could be approximated (with about 0.01% accuracy in the range $x \in [0, 10]$) by $f(x) = \exp[p(x)]$, where $p(x)$ is the fitted polynomial $p(x) = 1.11457 - 1.43361x - 0.0273053x^2 - 0.0287054x^3 + 0.00254457x^4 - 0.000133057x^5 - 3.04366\times10^{-6}x^6$.

The contact interaction energy in Eq. (15) is converted to a force between a plane and a sphere of radius r (AFM geometry) using the Derjaguin approximation $F(L) = 2\pi r G(L)$. That is, the corresponding force (normalised to r) is

$$F_{\text{contact}}(L)/r = \frac{4E_r\sigma_m}{15\sqrt{\pi}}\sqrt{\frac{\sigma_m}{R_r}}\exp\left(-\frac{L^2}{4\sigma_m^2}\right) f\left(\frac{L}{\sigma_m}\right). \tag{16}$$

A crude approximation to the Bessel functions can be obtained by taking the asymptote for $L \gg \sigma_m$,

$$F_{\text{contact}}(L)/r \approx \left(\frac{E_r 2\sqrt{2}}{5}\right)\frac{\sigma_m^4}{\sqrt{R_r}}\frac{e^{-L^2/2\sigma_m^2}}{L^2\sqrt{L}}. \tag{17}$$

In the region $L > 4\sigma_m$, this asymptote is about 80% accurate,[66] underestimating the exact expression by about 20%. In some studies the contact force has been represented by simple exponential decay.[39] But these analytic and asymptotic functions indicate that this is not a good approximation.

Fig. 3(a) shows the exact numerical elastic Hertzian contact force between two identically rough titania surfaces over a range of roughnesses. We observe that the elastic contact force becomes significant around $L \approx 4\sigma_m$, or more broadly between $3\sigma_m$ and $5\sigma_m$. Fig. 3(b) shows the impact of varying the asperity radius R with both surfaces having fixed roughness $\sigma = 2$ nm. Hertzian asperity contact becomes softer as the radius of the asperity cap becomes larger, that is, as the tip becomes more flat.

B. Amplification of exponentially decaying forces

Experimental surface forces are sometimes found to be well-characterised as an exponentially decaying force. Debye-Hückel theory predicts such a force (more precisely,

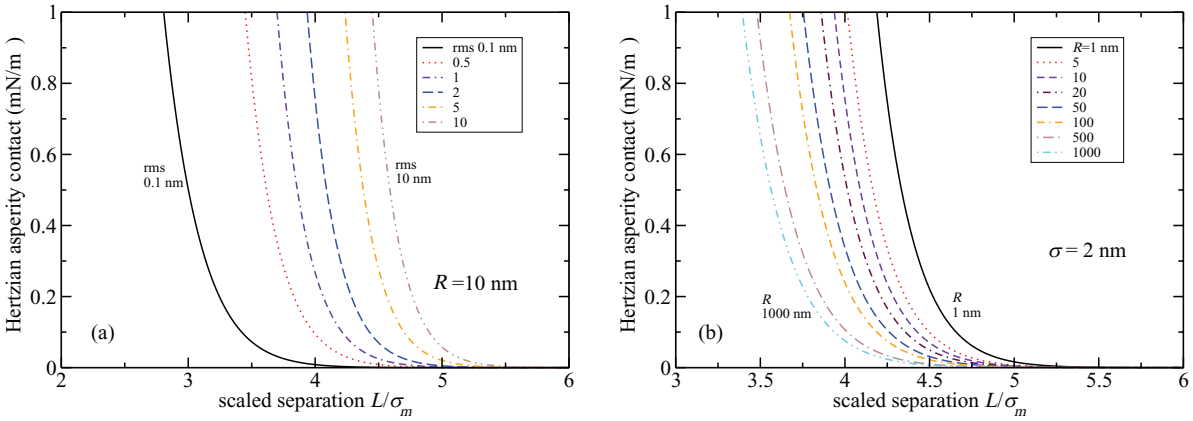

FIG. 3. Elastic contact force due to Hertzian compression of asperities with hemispherical caps, Eq. (14) between two rough titania surfaces ($E = 150$ GPa) at (a) various rms roughnesses (same rms for both surfaces) with the asperity radius of curvature $R = 10$ nm and (b) for various asperity radii R with roughness $\sigma = 2$ nm. Separations are scaled against mean roughness $\sigma_m = \sqrt{\sigma_1^2 + \sigma_2^2} = \sqrt{2}\sigma$.

This article is copyrighted as indicated in the article. Reuse of AIP content is subject to the terms at: http://scitation.aip.org/termsconditions. Downloaded to IP: 150.203.177.24 On: Wed, 23 Jul 2014 23:40:58

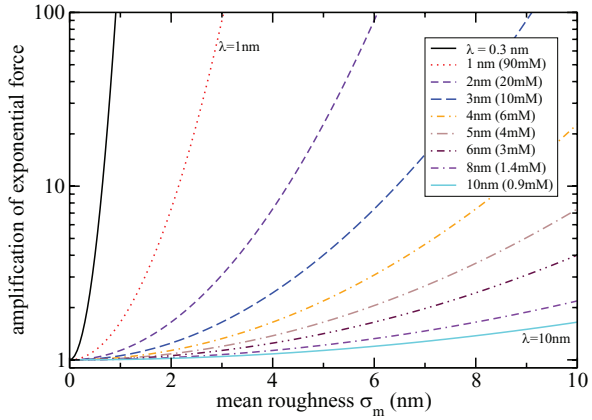

FIG. 4. Amplification factor $\exp(\sigma_m^2/2\lambda^2)$ for exponentially decaying forces $\exp(-L/\lambda)$ with various decay lengths λ as a function of the mean surface roughness $\sigma_m = \sqrt{\sigma_1^2 + \sigma_2^2}$. The quantity in parentheses in the legend indicates the concentration of 1:1 electrolyte which provides a Debye length equal to λ.

interaction energy) between smooth surfaces, $G_{\text{smooth}}(h) = G_0 \exp(-h/\lambda)$. The decay length λ is commonly given by the Debye length κ^{-1} (there may be deviations from this length due to specific adsorption of ions[53]).

The classic primary hydration force due to surface induced water structure also has such an exponential form.[54] But it should be noted that the physics of a real hydration force means that its amplitude G_0 would be attenuated under rough-surface conditions, which is not taken into account in this example. That is, the roughened hydration force under large rms roughness should be considered unphysical, since the surface induced water ordering responsible for the primary hydration force is disrupted by roughness.

Because of its relevance to DLVO (by way of Debye-Hückel theory) it is constructive to consider the analytic form of a roughened exponential interaction. Passing through Eq. (3), we obtain the approximate roughened interaction energy

$$G^{\text{exp}}(L) \approx G_0 e^{-L/\lambda} e^{\sigma_m^2/2\lambda^2} = G_{\text{smooth}}(L) \times \exp\left(\frac{\sigma_m^2}{2\lambda^2}\right). \tag{18}$$

(This is the asymptotic expression for $L \gg \sigma_m^2/\lambda$. The exact expression is given in the supplementary material[66]).

We see that the approximate amplification factor of exponential force between two rough surfaces is $\exp(\sigma_m^2/2\lambda^2)$. Amplification factors for exponentially decaying forces with various decay lengths are illustrated in Fig. 4 as a function of σ_r. With surface roughness no greater than 10 nm, the figure shows that while amplification may be great at high concentrations (100 mM and higher, with Debye lengths near 1 nm), it is negligible at low concentrations below 1 mM (with Debye lengths greater than 10 nm). Note however that for the very short Debye lengths found at high concentrations, the electrostatic force decays rapidly so the actual magnitude of the amplified force may still be very small.

III. ILLUSTRATIVE CALCULATIONS

A. Rough titania surface

We compare the performance of the roughness-averaged force against AFM measurements of the force between two titania surfaces[5] in the standard sphere-plane geometry. For simplicity, we consider identical surfaces. An AFM surface image is given in Fig. 5 along with the histogram of surface heights. The RMS roughness is $\sigma = 9.6$ nm. The histogram shows this surface has a relatively non-Gaussian distribution, allowing us to illustrate the difference between the two methods of modelling roughness, by histogram and by a Gaussian (RMS) model.

AFM force measurements were undertaken at pH 9 in 1 mM NaCl salt solution. For simplicity we use routine DLVO theory (a nonlinear Poisson-Boltzmann model plus nonretarded surface van der Waals) with constant surface charge to generate theoretical smooth surface forces, neglecting additional nonelectrostatic contributions such as ionic dispersion forces,[55] ion size, or surface charge regulation.[56] The Hamaker constant for the surface van der Waals force (non-retarded Casimir-Lifshitz force) was taken to be $A = 14.6kT$, calculated from the average dielectric function of titania[57] and water.[58] Young's modulus for titania is[5] $E = 150$ GPa.

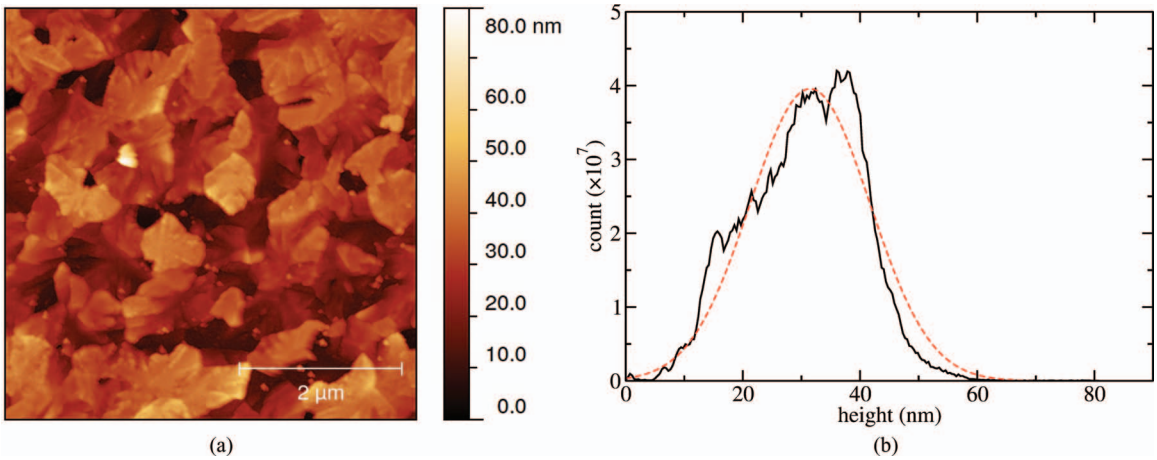

FIG. 5. (a) AFM surface images of a titania surface with RMS roughness $\sigma = 9.6$ nm. (b) Histogram of surface heights. The solid black curve marks the AFM measurement, the red dashed curve shows the best Gaussian fit.

This article is copyrighted as indicated in the article. Reuse of AIP content is subject to the terms at: http://scitation.aip.org/termsconditions. Downloaded to IP: 150.203.177.24 On: Wed, 23 Jul 2014 23:40:58

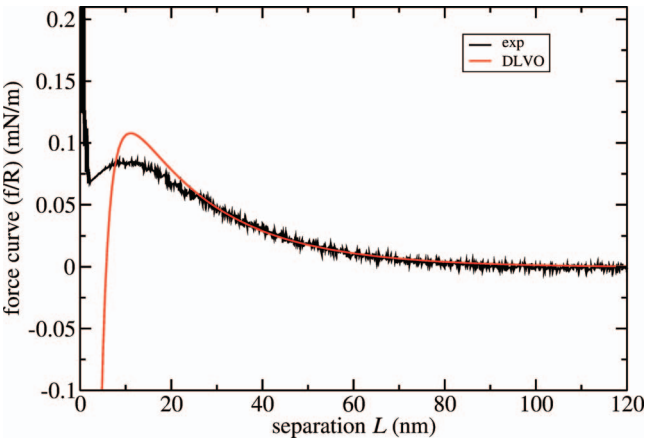

FIG. 6. Conventional experimental AFM force curve for a rough titania surface (rms ≈ 9.67 nm), with the best conventional DLVO fit (surface charge −0.0007 C m^{-2}, surface potential −35 mV, NaCl concentration 0.18 mM) "conventional" here means that roughness is not accounted for, and the repulsive contact wall is placed at $L = 0$.

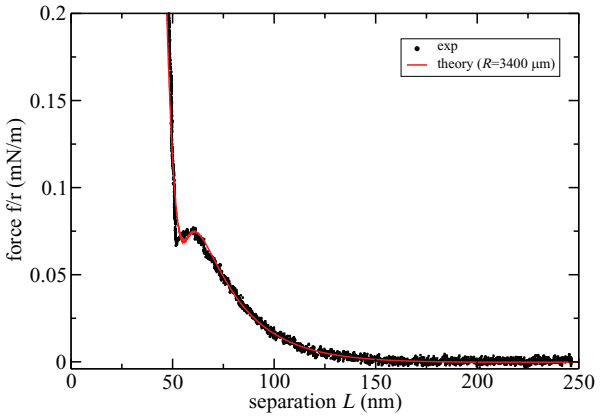

FIG. 7. Roughened theoretical force curve (including elastic contact) fitted against experimental AFM measurement of the force between two rough titania surfaces in 0.18 mM NaCl at pH 9. DLVO calculations are taken with constant surface charge. Hertzian radius of asperity tips is $R = 3400$ μm. Surface charge −0.0025 C m^{-2} (surface potential −64 mV on isolated surfaces).

The conventional experimental force measurement and DLVO fit,[5] without consideration of roughness (such that the contact wall is placed at $L = 0$) are shown in Fig. 6. The probe was a borosilicate sphere coated with an 82 nm layer of titania, total sphere radius 10.6 μm. The flat substrate was a boron-doped silicon wafer with a native oxide layer, also coated with an 82 nm layer of titania.[5] The best conventional DLVO fit corresponded to surface charge −0.0007 C m^{-2} with a decay length corresponding to an ionic strength of 0.18 mM. The corresponding surface potential is −35 mV, somewhat lower in magnitude than the −50 or −60 mV one would expect from zeta potential measurements[5]). The problem of roughness is apparent in this figure. The experimental data are characterised by a force peak of about 0.085 mN/m located 10 nm out from the contact wall, together with a contact force of 0.068 mM/N. No set of DLVO parameters (surface charge and concentration) is able to capture this contact force simultaneously with the short range peak while at the same time fitting the long range decay curve. The best DLVO fit predicts a higher peak of 0.1 mN/m and predicts that the force becomes adhesive at surface separations less than 6 nm (due to the van der Waals interaction), whereas the measured force remains repulsive at contact.

In Fig. 7 we compare the experimental force curve present against theoretical roughened force curve, applying Eq. (7) (using the AFM histogram of surface heights) to both the DLVO noncontact interaction and the contact interaction of Hertzian sphere compression Eq. (14). Very good agreement is found, obtained by fitting both the DLVO surface charge to −0.0025 C m^{-2} (potential −64 mV, consistent with zeta potential measurements[5]) with NaCl concentration 0.18 mM together with asperity tip radius $R = 3400$ μm. This very large radius indicates that the tips of asperities are nearly flat. The long range decay rate of the force remains constant, as anticipated by Eq. (18). The fitting procedure involves realignment of the raw experimental data to adjust compliance against the elastic contact force. That is both theory and experiment depend on one another and the fitted parameters are adjusted iteratively until a sufficiently self-consistent match is obtained.

In the supplementary material[66] we present an alternative model of elastic contact invoking elastic bending of asperities, controlled by the average cross-sectional area of asperities. This model can provide a fit equivalent to the one we obtained with Hertzian contact if the cross-sectional area is taken to be 44 Å^2. This implies asperities of very high aspect ratio (tall height relative to a small diameter). But the AFM image in Fig. 5 suggests that asperities on this surface do not have such high aspect ratio. It is more reasonable to adopt our Hertzian model of asperities with relatively flat tips.

B. General effects of roughness

We use the final DLVO parameters established for the rough titania surface above to explore the general effect that roughness exerts, compared to the conventional DLVO force. The salt solution is 0.18 mM NaCl (Debye length 22.6 nm), titania surface charge is −0.0025 C m^{-2} (yielding a surface potential of −64 mV on isolated surfaces).

We first consider the effect of varying the RMS roughness on the noncontact forces (without elastic contact) which comprise DLVO forces, that is the attractive Hamaker-van der Waals force and the repulsive force due to formation of the electrolytic diffuse layer. The effect of roughness on these two DLVO components is shown in Fig. 8. Since a Debye length of 22.6 nm is quite large, amplification of electrolytic repulsion, Fig. 8(a) is relatively mild until roughness becomes greater than 10 nm (cf. Fig. 4). The amplification by roughness of the shorter range attractive Hamaker force, Fig. 8(b), is however large and significant even with roughness as low as 1.5 nm. This observation is consistent with the effect of roughness on the Casimir force calculated using the proximity force approximation.[59]

The total DLVO force is shown in Fig. 9(a). The effect of roughness becomes apparent once the rms roughness exceeds 1 nm. The long range behaviour appears unperturbed by roughness. But amplification of the short range attractive

This article is copyrighted as indicated in the article. Reuse of AIP content is subject to the terms at: http://scitation.aip.org/termsconditions. Downloaded to IP: 150.203.177.24 On: Wed, 23 Jul 2014 23:40:58

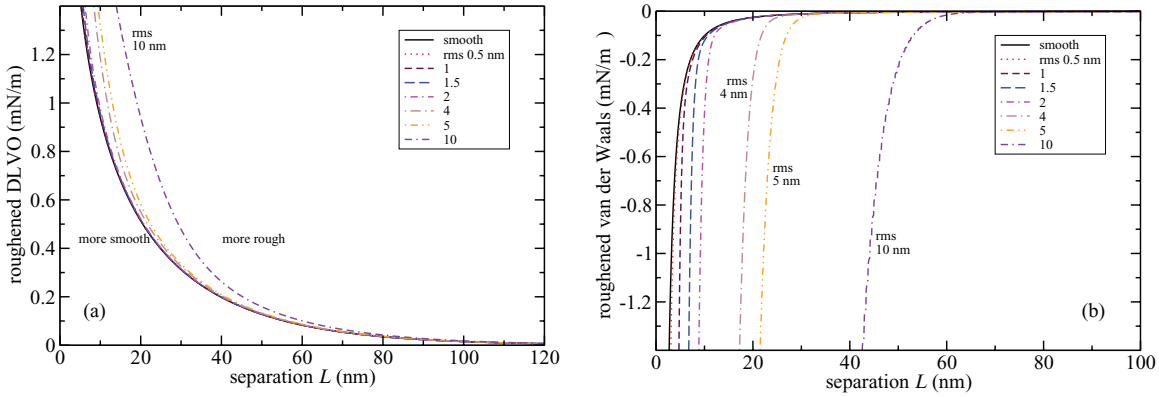

FIG. 8. Roughened force curves derived from the component DLVO force curves of titania in 0.18 mM NaCl with constant surface charge -0.0025 C m^{-2} (surface potential -64 mV on isolated surfaces). (a) electrolytic (non van der Waals) and (b) van der Waals component.

Hamaker force means that the repulsive peak in the total force is progressively lost as roughness increases.

The contact wall will move outwards as roughness increases, but its strength also depends on the curvature of asperity tips (see Fig. 3). The combination of the contact force with the amplified short-range van der Waals attraction will in general form a primary attractive well. When the contact wall is sufficiently strong (high rms roughness or low radius of curvature of asperity tips), it cuts off the stronger van der Waals interaction found at shortest separations, such that the magnitude of the attractive well becomes shallower as roughness increases. The overall observed force between rough surfaces might be interpreted as "loss" of van der Waals attraction. In fact van der Waals attraction is strengthened by roughness (Figs. 8(b) and 9(a)). The loss of overall attraction occurs due to an increase in the repulsive elastic contact force.

C. Histogram vs Gaussian RMS

The calculations made for the rough surface in Sec. III A above were made using the experimental AFM histogram. The difference between this histogram and a Gaussian distribution with the same rms roughness, $\sigma = 9.67$ nm, can be seen in Fig. 5(b). In Fig. 10 we compare the full roughened force calculated by histogram and by Gaussian rms, using the same surface charge and asperity curvature established in Sec. III A. The non-normal distribution found in this histogram provides a greater proportion of asperities which are longer than average. Consequently the histogram qualitatively behaves like a system with a larger rms value. The elastic contact wall is stronger and pushed outwards, and the short range van der Waals attraction is more greatly amplified, such that the peak near $L = 60$ nm is reduced in height.

Significantly, since the Gaussian distribution loses the bias towards longer asperities, the magnitude of the contact wall is reduced (with the same Hertzian radius retained in both cases). The contact wall of the Gaussian distribution is located at $L = 23$ nm and is nearly vertical, compared to the softer contact wall near $L = 45$ nm for the non-normal histogram. The interaction exhibits strong adhesion at the contact wall under the Gaussian distribution. We conclude that where the surface follows a non-normal distribution of heights, this property must not be neglected.

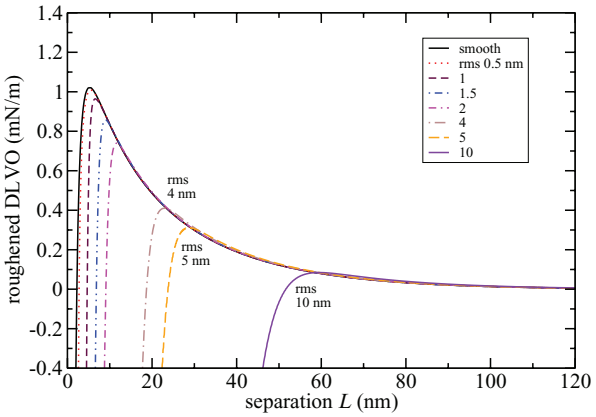

FIG. 9. Roughened noncontact force curves derived from the DLVO force curve of titania in 0.18 mM NaCl with constant surface charge -0.0025 C m^{-2} (surface potential -64 mV on isolated surfaces), for a range of rms roughnesses.

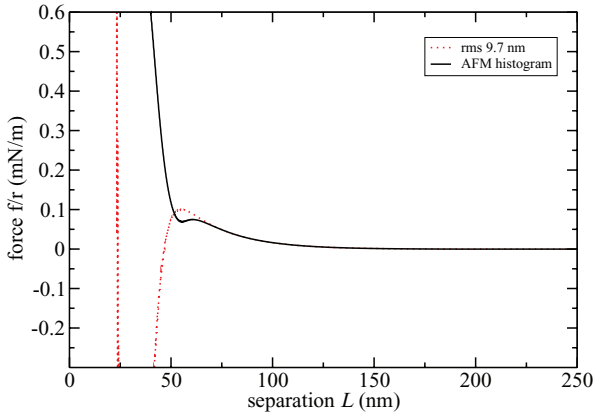

FIG. 10. Comparison of roughness described by an experimental histogram (solid black curve) and by the corresponding Gaussian RMS 9.6 nm (dotted red curve). Roughened force curves derived from the DLVO force curve of titania in 0.18 mM NaCl with constant surface charge -0.0025 C m^{-2} (surface potential -64 mV on isolated surfaces). Elastic contact is given by Hertzian contact of asperity tips with radius of curvature $R = 3400$ μm.

This article is copyrighted as indicated in the article. Reuse of AIP content is subject to the terms at: http://scitation.aip.org/termsconditions. Downloaded to IP: 150.203.177.24 On: Wed, 23 Jul 2014 23:40:58

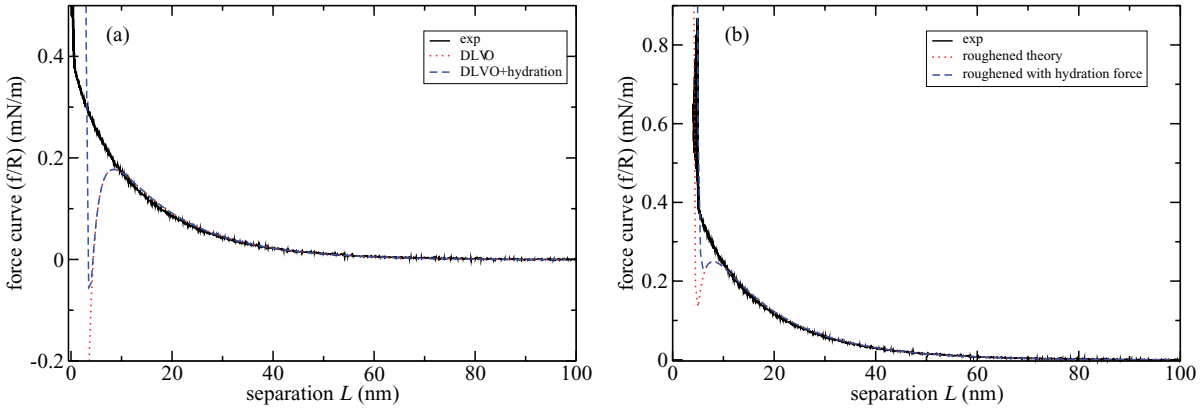

FIG. 11. Experimental AFM and theoretical force curves between titania surfaces in 0.38 mM NaCl. The black curve indicates experimental data. (a) The dotted red curve indicates the traditional analysis with contact wall at $L = 0$ and classic DLVO theory (surface charge -0.0012 C m^{-2}, surface potential -26 mV). (b) The dotted red curve indicates the roughened model (surface charge -0.0014 C m^{-2}, surface potential -30 mV) with Hertzian asperity contact ($R = 4$ nm). The dashed blue curve adds an hydration force ($F_0 = 20$ N/m, $\lambda = 0.3$ nm), smooth in (a), roughened in (b).

D. Smooth titania surface

In Fig. 11 we present experimental and theoretical forces for a smooth titania surface similar to that reported in Ref. 5. The probe was a borosilicate sphere coated with a 102 nm layer of titania, total sphere radius 10.3 μm. The flat substrate was a boron-doped silicon wafer with a native oxide layer, also coated with a 102 nm layer of titania.[5] The two surfaces in contact have a slightly asymmetric roughness, rms 0.83 nm (sphere) and 0.62 nm (flat), giving a combined roughness $\sigma_m = 1.04$ nm. The traditional unroughened DLVO fit of the data, placing the contact wall at $L = 0$, is shown in Fig. 11(a) (surface charge -0.0012 C m^{-2}, surface potential -26 mV). At small separations below 1 nm a typical van der Waals turnaround leading to attraction at contact is found in the DLVO curve. No such short range peak is seen in the experimental data, which is repulsive at all separations.

Invoking the elastic contact model with asperity curvature $R = 4$ nm, we improve the discrepancy by pulling the contact forward to 5 nm, Fig. 11(b). Contact adhesion is thereby removed by the asperity contact wall, though a short range repulsive peak remains. The match between theory and experiment can be improved further by adding other noncontact forces missing from basic DLVO theory such as the hydration force due to surface-induced water structure.[54] The theoretical roughened curve, enhanced with a typical exponentially decaying hydration force with amplitude 20 N/m and decay length 0.3 nm, is also shown in Fig. 11(b). The hydration force is added to the smooth noncontact force and is therefore amplified by roughening. We find it helps close the gap between the repulsive wall and the short range peak.

The rms roughness could potentially be treated as a fitting parameter, in which case the experimental curve could be fitted precisely with a larger rms roughness. But we are inclined to consider the AFM measurement of rms roughness to be reliable, such that the original smooth surface roughnesses of 0.62 and 0.83 nm should be trusted. We therefore interpret the remaining discrepancy between theory and experiment in Fig. 11(b) as a question of how accurately the noncontact force between smooth surfaces has been described. We have already shown that a primary hydration force helps close the gap. Further short range repulsion could also be added by taking a van der Waals attraction with a finite value at contact,[60] or via nonelectrostatic ion interactions in combination with surface-induced water structure (secondary hydration force)[61] or in combination with surface charge regulation.[56]

IV. DISCUSSION

A. Elastic contact wall and apparent zero

Our elastic contact model typically showed a repulsive barrier exceeding a force of 1 mN/m at a separation $L_0 = 3$–$5\sigma_m$, see Fig. 3. We interpret this contact location as the "apparent zero" found by AFM force measurement. The standard atomic force microscope is unable to measure absolute distances between surfaces, and the question of the "apparent zero" has been a vexing one.

The proportion $p(L_0)$ of surface asperities in contact at the apparent zero may be given by the cumulative probability function, $p(L_0) = \int_{L_0}^{\infty} dh\, P(h)$. Assuming a Gaussian distribution of heights, this is given by the standard normal cumulative distribution function. If $L_0 = 4\sigma$, then the proportion of the surface in contact is as low as 0.003%.

B. Elastic contact as apparent hydration force

Aside from relocating the "apparent zero" to $L_0 = 3$–5σ, we see, for instance in Fig. 3, that the elastic contact force is not vertical. That is, the contact wall at L_0 is a soft wall, not a hard wall, and some contact repulsion extends out beyond L_0 due to a small number of very long asperities. If one were to model contact with a simple hard wall at L_0, then one would find a short range repulsive force not modelled by DLVO theory, due to the soft toe of the elastic contact force. This soft contact force extends out from L_0 over a distance of around $\sigma_m\sqrt{2}$, the Gaussian decay length seen in the asymptotic formula, Eq. (17).

This scenario is reminiscent of repulsive non-DLVO forces often described as "hydration forces."[39,62–65] In the case of molecularly smooth surfaces such as mica, the short-range repulsion may well be a true hydration force.[54] Short range repulsion found in soft membranes could be attributed

This article is copyrighted as indicated in the article. Reuse of AIP content is subject to the terms at: http://scitation.aip.org/termsconditions. Downloaded to IP: 150.203.177.24 On: Wed, 23 Jul 2014 23:40:58

to height fluctuations in the membrane surface, a dynamic cousin of roughness.[31] In other cases, though, it may prove more appropriate to interpret such non-DLVO forces not as a hydration force but as a soft contact force due to the contact of asperities of rough surfaces. The hydration force has been employed as an exponentially decaying force[39,54,63] and roughness has been modelled in the same fashion.[39] Our analytical formula in Eq. (16) provides an alternative form which should prove more successful at modelling roughness than an exponential form. Our contact forces could be crudely approximated by an exponential with decay length $\sigma/4$, but the combination of Gaussian and $L^{-5/2}$ decay means the real elastic contact forces decay more quickly than an exponential function.

C. Scheme for exploitation

A simple, approximate implementation to account for roughness in force versus separation data or for a theoretical force would involve the following steps.

1. Determine the roughness of the surfaces by atomic force microscopy expressed either as RMS values σ_1, σ_2 or as histograms.
2. Implement the effect of roughness in the contact region with $\sigma_m^2 = \sigma_1^2 + \sigma_2^2$ using Eq. (16) for the contact force. This determines how the separation changes with applied force during contact (the compliance). $R_r \approx 4\sigma_m$ may serve as an initial guess for the reduced curvature of asperity tips.
3. Over the appropriate loading, equate the compliance of the experimental data to the compliance calculated in Step 2. This also inherently corrects the experimental data for the offset in separation due to roughness.
4. Include the roughened noncontact interaction for a given surface charge (or surface potential) by implementing Eq. (8). The noncontact force is capped at its contact value $F(0)$, see Eq. (10). If mean surface roughness is characterised by σ_m then a satisfactory histogram can be constructed from the Gaussian distribution using 501 points spread between $-10\sigma_m$ and $10\sigma_m$.
5. Iteratively adjust the compliance and surface separation together with the surface charge or potential as the non-contact force will influence the zero of separation through changes in the compliance.

For smoother surfaces the basic contact force with $R_r = 4\sigma_m$ in Step 2 may be too soft. Increase the strength of the contact force by decreasing R_r. Rougher surfaces may require a softer contact force, achieved by increasing R_r.

V. CONCLUSIONS

Our model of surface roughness combines two chief elements. First, a flat-surface force is convoluted (averaged) over the distribution of surface heights (which can be represented either by a histogram or by a normal Gaussian distribution with a given rms roughness). Second we add a force due to the elastic contact of surface asperities.

The general impact of averaging a noncontact (DLVO) force over a roughness profile is to amplify the short-range behaviour of the force. For instance, any van der Waals force which provides adhesion at short range will be amplified, which may have the consequence of eroding any repulsive peak that lies between the short-range adhesive and mid-range repulsive regimes. Roughness is found to preserve the decay rate of exponentially decaying forces, amplifying them by a factor of $\exp(\sigma^2/\lambda^2)$ per surface.

We represent elastic contact as Hertzian compression of hemispherical caps of asperities. This requires the average radius of curvature of asperity tips to be determined. We obtained an explicit expression for the elastic contact models, scaling against the mean roughness $\sigma_m^2 = \sigma_1^2 + \sigma_2^2$. We found a real rough titania surface (rms $\approx$ 9.67 nm) to be best modelled by asperity tip curvatures of $R = 3400$ μm, indicating the tips of asperities are nearly flat. A smooth titania surface (rms $\approx$ 0.7 nm) was best modelled by Hertzian spherical asperity compression with asperity radius $R = 4$ nm.

The elastic contact force provides a repulsive force which has the general impact of pushing the repulsive contact wall detected in surface force measurements out from the average contact position $L = 0$ to a position that scales with the RMS roughness of the surfaces ($L \approx 4\sigma_m$).

ACKNOWLEDGMENTS

We acknowledge the support of the Australian Research Council's Discovery Projects funding scheme.

[1] B. Derjaguin and L. Landau, Acta Physicochim. URSS **14**, 633 (1941) [republished in Prog. Surf. Sci. **43**, 30 (1993)].
[2] E. J. W. Verwey and J. T. G. Overbeek, *Theory of the Stability of Lyophobic Colloids* (Elsevier Publishing Company, 1948).
[3] D. F. Parsons, M. Boström, P. L. Nostro, and B. W. Ninham, Phys. Chem. Chem. Phys. **13**, 12352 (2011).
[4] D. Grasso, K. Subramaniam, M. Butkus, K. Strevett, and J. Bergendahl, Rev. Environ. Sci. Biol./Technol. **1**, 17 (2002).
[5] R. B. Walsh, A. Nelson, W. M. Skinner, D. Parsons, and V. S. J. Craig, J. Phys. Chem. C **116**, 7838 (2012).
[6] T. Missana and A. Adell, J. Colloid Interface Sci. **230**, 150 (2000).
[7] E. I. Benítez, D. B. Genovese, and J. E. Lozano, Food Hydrocolloids **21**, 100 (2007).
[8] M. Michalski, S. Desobry, V. Babak, and J. Hardy, Colloids Surf., A **149**, 107 (1999).
[9] A. Nosrati, J. Addai-Mensah, and W. Skinner, Chem. Eng. J. **152**, 406 (2009).
[10] J. S. Buckley, K. Takamura, and N. R. Morrow, SPE Reservoir Eng. **4**, 332 (1989).
[11] S. E. Truesdail, J. Lukasik, S. R. Farrah, D. O. Shah, and R. B. Dickinson, J. Colloid Interface Sci. **203**, 369 (1998).
[12] M. A.-S. Vigeant, R. M. Ford, M. Wagner, and L. K. Tamm, Appl. Environ. Microbiol. **68**, 2794 (2002).
[13] Y.-I. Chang and P.-K. Chang, Colloids Surf., A **211**, 67 (2002).
[14] R. A. Curtis, A. Montaser, J. M. Prausnitz, and H. W. Blanch, Biotechnol. Bioeng. **58**, 451 (1998).
[15] J. Nalaskowski, S. Veeramasuneni, J. Hupka, and J. Millers, J. Adhes. Sci. Technol. **13**, 1519 (1999).
[16] R. F. Considine and C. J. Drummond, Langmuir **17**, 7777 (2001).
[17] M. Valtiner, K. Kristiansen, G. W. Greene, and J. N. Israelachvili, Adv. Mater. (Weinheim, Ger.) **23**, 2294 (2011).
[18] R. Jones, H. M. Pollock, J. A. S. Cleaver, and C. S. Hodges, Langmuir **18**, 8045 (2002).
[19] P. J. van Zwol, G. Palasantzas, and J. T. M. De Hosson, Appl. Phys. Lett. **91**, 101905 (2007).
[20] P. J. van Zwol, G. Palasantzas, M. van de Schootbrugge, and J. T. M. De Hosson, Appl. Phys. Lett. **92**, 054101 (2008).

This article is copyrighted as indicated in the article. Reuse of AIP content is subject to the terms at: http://scitation.aip.org/termsconditions. Downloaded to IP: 150.203.177.24 On: Wed, 23 Jul 2014 23:40:58

[21]L. D. Landau and E. M. Lifshitz, *Theory of Elasticity*, 5th ed., Theoretical Physics Vol. VII (Fizmatlit, Moscow, 2007) (in Russian).
[22]N. A. Burnham, R. J. Colton, and H. M. Pollock, J. Vac. Sci. Technol., A **9**, 2548 (1991).
[23]P. Attard and J. L. Parker, Phys. Rev. A: At., Mol., Opt. Phys. **46**, 7959 (1992).
[24]K. L. Johnson, K. Kendall, and A. D. Roberts, Proc. R. Soc. London, Ser. A **324**, 301 (1971).
[25]B. Derjaguin, V. Muller, and Y. Toporov, J. Colloid Interface Sci. **53**, 314 (1975).
[26]D. Tabor, J. Colloid Interface Sci. **58**, 2 (1977).
[27]D. Maugis, J. Colloid Interface Sci. **150**, 243 (1992).
[28]B. Derjaguin, Kolloid-Z. **69**, 155 (1934) (in German).
[29]L. R. White, J. Colloid Interface Sci. **95**, 286 (1983).
[30]S. Bhattacharjee, J. Y. Chen, and M. Elimelech, Colloids Surf., A **165**, 143 (2000).
[31]E. Schneck and R. R. Netz, Curr. Opin. Colloid Interface Sci. **16**, 607 (2011).
[32]S. Bhattacharjee, C.-H. Ko, and M. Elimelech, Langmuir **14**, 3365 (1998).
[33]J. F. L. Duval, F. A. M. Leermakers, and H. P. van Leeuwen, Langmuir **20**, 5052 (2004).
[34]E. M. Hoek and G. K. Agarwal, J. Colloid Interface Sci. **298**, 50 (2006).
[35]X. Huang, S. Bhattacharjee, and E. M. V. Hoek, Langmuir **26**, 2528 (2010).
[36]C. Shen, L.-P. Wang, B. Li, Y. Huang, and Y. Jin, "Role of Surface Roughness in Chemical Detachment of Colloids Deposited at Primary Energy Minima," Vadose Zone J. **11** (2012).
[37]S. Shulepov and G. Frens, J. Colloid Interface Sci. **170**, 44 (1995).
[38]C. Henry, J.-P. Minier, G. Lefèvre, and O. Hurisse, Langmuir **27**, 4603 (2011).
[39]M. Valtiner, X. Banquy, K. Kristiansen, G. W. Greene, and J. N. Israelachvili, Langmuir **28**, 13080 (2012).
[40]L. Suresh and J. Y. Walz, J. Colloid Interface Sci. **183**, 199 (1996).
[41]R. S. Decca, E. Fischbach, G. L. Klimchitskaya, D. E. Krause, D. López, and V. M. Mostepanenko, Phys. Rev. D: Part. Fields **68**, 116003 (2003).
[42]R. R. Dagastine, M. Bevan, L. R. White, and D. C. Prieve, J. Adhes. **80**, 365 (2004).
[43]P. J. van Zwol, V. B. Svetovoy, and G. Palasantzas, Phys. Rev. B: Condens. Matter Mater. Phys. **80**, 235401 (2009).
[44]W. Broer, G. Palasantzas, J. Knoester, and V. B. Svetovoy, Phys. Rev. B: Condens. Matter Mater. Phys. **85**, 155410 (2012).
[45]B. Persson, Surf. Sci. Rep. **61**, 201 (2006).
[46]U. Mahajan, M. Bielmann, and R. K. Singh, Electrochem. Solid-State Lett. **2**, 46 (1999).
[47]F. Chen, U. Mohideen, G. L. Klimchitskaya, and V. M. Mostepanenko, Phys. Rev. A: At., Mol., Opt. Phys. **66**, 032113 (2002).
[48]P. J. van Zwol, G. Palasantzas, and J. T. M. De Hosson, Appl. Phys. Lett. **91**, 144108 (2007).
[49]H.-J. Butt, Langmuir **24**, 4715 (2008).
[50]K. L. Johnson, *Contact Mechanics* (Cambridge University Press, Cambridge, 1985).
[51]T. N. Krupenkin, J. A. Taylor, T. M. Schneider, and S. Yang, Langmuir **20**, 3824 (2004).
[52]J. Groten and J. Rühe, Langmuir **29**, 3765 (2013).
[53]R. Pashley and J. Quirk, Colloids Surf. **9**, 1 (1984).
[54]S. Marčelja and N. Radić, Chem. Phys. Lett. **42**, 129 (1976).
[55]D. F. Parsons and B. W. Ninham, J. Phys. Chem. C **116**, 7782 (2012).
[56]V. Deniz and D. F. Parsons, J. Phys. Chem. C **117**, 16416 (2013).
[57]L. Bergström, Adv. Colloid Interface Sci. **70**, 125 (1997).
[58]R. R. Dagastine, D. C. Prieve, and L. R. White, J. Colloid Interface Sci. **231**, 351 (2000).
[59]P. J. van Zwol, G. Palasantzas, and J. T. M. De Hosson, Phys. Rev. B **77**, 075412 (2008).
[60]L. R. White, J. Colloid Interface Sci. **343**, 338 (2010).
[61]D. F. Parsons and B. W. Ninham, Colloids Surf., A **383**, 2 (2011).
[62]R. Pashley, J. Colloid Interface Sci. **80**, 153 (1981).
[63]J.-P. Chapel, Langmuir **10**, 4237 (1994).
[64]J. Valle-Delgado, J. Molina-Bolívar, F. Galisteo-González, and M. Gálvez-Ruiz, Curr. Opin. Colloid Interface Sci. **16**, 572 (2011).
[65]V. Parsegian and T. Zemb, Curr. Opin. Colloid Interface Sci. **16**, 618 (2011).
[66]See supplementary material at http://dx.doi.org/10.1063/1.4871412 for further discussion of asymptotic behaviour and alternative models of elastic contact (beam compression and bending).

This article is copyrighted as indicated in the article. Reuse of AIP content is subject to the terms at: http://scitation.aip.org/termsconditions. Downloaded to IP: 150.203.177.24 On: Wed, 23 Jul 2014 23:40:58